SAE TECHNICAL PAPER SERIES

2006-01-0229

Effects of Combustion Phasing, Relative Air-fuel Ratio, Compression Ratio, and Load on SI Engine Efficiency

Ferrán A. Ayala, Michael D. Gerty and John B. Heywood
Sloan Automotive Laboratory, Massachusetts Institute of Technology

ACHIEVED TRANSACTIONS

Reprinted From: SI Combustion and Direct Injection SI Engine Technology (SP-2016)

ISBN 0-7680-1636-3

9 780768 016369

2006 SAE World Congress
Detroit, Michigan
April 3-6, 2006

SAE International™

400 Commonwealth Drive, Warrendale, PA 15096-0001 U.S.A. Tel: (724) 776-4841 Fax: (724) 776-5760 Web: www.sae.org

The Engineering Meetings Board has approved this paper for publication. It has successfully completed SAE's peer review process under the supervision of the session organizer. This process requires a minimum of three (3) reviews by industry experts.

ISSN 0148-7191

Printed in USA

2006-01-0229

Effects of Combustion Phasing, Relative Air-fuel Ratio, Compression Ratio, and Load on SI Engine Efficiency

Ferrán A. Ayala, Michael D. Gerty and John B. Heywood
Sloan Automotive Laboratory, Massachusetts Institute of Technology

ABSTRACT

In an effort to both increase engine efficiency and generate new, consistent, and reliable data useful for the development of engine concepts, a modern single-cylinder 4-valve spark-ignition research engine was used to determine the response of indicated engine efficiency to combustion phasing, relative air-fuel ratio, compression ratio, and load. Combustion modeling was then used to help explain the observed trends, and the limitations on achieving higher efficiency. This paper analyzes the logic behind such gains in efficiency and presents correlations of the experimental data. The results are helpful for examining the potential for more efficient engine designs, where high compression ratios can be used under lean or dilute regimes, at a variety of loads.

Extensive data from this study, across a wide range of engine operating conditions, show that the well-known loss of Net Indicated Mean Effective Pressure (NIMEP; the ratio of net work per cycle to cylinder volume displaced per cycle), with spark retard varies with operating conditions, mostly from variations in burn durations. However, a combustion phasing parameter, here termed “combustion retard”, which represents the shift of the crank angle for 50% mass fraction burned from the optimal angle, was found to correlate with high accuracy all the changes in indicated torque output.

At the baseline compression ratio of 9.8:1, as the engine was operated under mid-load and increasing relative air-fuel ratio, the efficiency curve versus dilution showed two distinct regimes. Through the first regime, efficiency increased with dilution until it peaked at a certain relative air-fuel ratio (range 1.5 to 1.6). Beyond this peak efficiency ratio began a second regime characterized by a falling efficiency due to increasing combustion duration and variability. Modeling and data analysis were used to investigate the contributions of pumping losses, mixture composition (ratio of specific heats), heat loss, burn durations, and combustion variability to the overall efficiency trend. It was determined that the leveling off in efficiency at high air-fuel ratios is due to a lengthening of burn duration beyond a critical value (10-90% burn angle of 30 degrees). Increasing compression ratio increases flame speed, extending the air-fuel ratio for peak efficiency an additional 0.1 lambda. Increasing combustion variability only affects the downward slope in efficiency at high air/fuel ratios. Increasing load extends the peak efficiency to leaner conditions.

Above a compression ratio of 9.8:1, relative mid-load net efficiency improvement is about 2.5% per unit compression ratio. Efficiency peaks at a compression ratio of about 15:1 with a maximum benefit of 6-7%. Efficiency improves more with compression ratio at high speeds and loads due to the reduced importance of heat loss. Wide-open throttle indicated torque at MBT spark timing behaves similarly to mid-load efficiency, with a maximum benefit of 8-9% at a 14:1 compression ratio. These data are particularly useful considering the limited available publications containing consistent compression ratio effect data for a wide range of operating conditions.

Relative net efficiency improvement from increasing load is about 6% per bar net indicated mean effective pressure at mid-load. About 80% of the improvement is from reduced pumping losses and 20% is from heat loss becoming a smaller portion of the overall charge energy. Correlations of efficiency with load are also presented.

INTRODUCTION

With today’s high oil prices, the increasing global warming effects from fossil fuel emissions, and the unavailability of better substitutes for the internal combustion engine for at least another 15 to 20 years, increasing engine efficiency continues to be one of the most relevant topics in the auto industry. There is an ongoing emphasis on the traditional methods for obtaining higher engine efficiency such as boosting and increasing the compression ratio, as well as a growing interest in the development of newer approaches such as lean engine concepts. For these reasons, the availability of up-to-date, reliable efficiency data and well-behaved correlations across a variety of operating conditions continues to be essential for the engine research and development process. In particular, a better understanding of the effect of combustion phasing and load on efficiency is important as one tries to benefit from boost, while avoiding knock; fundamental knowledge of the effect of air-fuel ratio on efficiency is essential to develop successful lean, and hydrogen-enhanced engines; advantages and diminishing returns of using higher compression ratio is also important.

Surprisingly, there is scant efficiency data available in publications. This data is rather old, and only covers limited operating conditions. For example, the most consistent set of efficiency data for various compression ratios is almost 20 years old [5]. Revisiting this area and generating a consistent set of data and correlations under a diverse set of engine conditions is important to validate past results, and aid in engine design. By presenting practical correlations, and fundamental explanations, this paper focuses on the effects of combustion phasing, air-fuel ratio, compression ratio, and load, on engine efficiency.

EXPERIMENTAL METHOD

SETUP

The engine used for this study is a Ricardo Hydra MK III with baseline compression ratio of 9.8:1. The original head has been replaced with a B5254 Volvo head that has a modern 4-valve pentroof combustion chamber with a central spark plug. The engine has relatively low swirl and high tumble. Turbulence is increased with a charge motion control plate added to the intake manifold [1, 4]. The engine is naturally aspirated, and air supply from a compressor is used to simulate boost. Two other compression ratios were used with this engine, 11.6:1 and 13.4:1. Engine details are shown in Table 1.

Table 1 – Engine Specifications

Displaced Volume (cm^3)	487
Clearance Volume (cm^3)	46
Bore (mm)	83
Stroke (mm)	90
Connecting Rod Length (mm)	158
Piston 1 Clearance Vol. (cm^3)/Rc	55 / 9.8:1
Piston 2 Clearance Vol. (cm^3)/Rc	46 / 11.6:1
Piston 3 Clearance Vol. (cm^3)/Rc	39 / 13.4:1
Valve timing	IVC 60º ABDC IVO 0º ATDC
	EVO 8º ATDC EVO 68º BBDC

The relative air-fuel ratio was measured in the exhaust using a wideband Horiba MEXA-110 lambda sensor. The pressure inside the cylinder was measured using a Kiestler 60125A piezoelectric pressure transducer.

EXPERIMENTAL PROCEDURE

Combustion Retard

To determine the relationship between spark retard and engine output, a series of experiments were performed where MBT timing was first located for a specified load, and then the spark was advanced or retarded about optimum timing. While doing each spark sweep the fuel flow was kept constant. The spark was first advanced 2º to 6º CA before MBT until the knock limit was reached, setting the spark advance limit; the spark was then retarded in steps of 2º CA until either the combustion process became unstable (COV of NIMEP > 3%) or the exhaust temperature got too high (>750 ºC), setting the spark retard limit. This procedure was repeated for a range of target loads (8 to 15 bar), for three different compression ratios (9.8, 11.6, 13.4), for three different dilution levels (λ=1, λ=1.3, λ=1.6), for three different enhancement levels (0%, 15%, 30%), and for two different fuels (toluene and PRF 120). Enhancement refers to the addition of a hydrogen-rich mixture to the engine to speed up the combustion process. The level of enhancement is a measure of the proportion of the total fuel going into the system that is reformed or converted into this hydrogen-rich mixture, also called plasmatron reformate [3]. The engine was run naturally aspirated or boosted as needed, to achieve the desired target load at the given operating conditions.

Air-fuel ratio, Load, and Compression Ratio

Two sets of experiments were performed to explore the effect of air-fuel ratio on efficiency. The first set of experiments was used to understand the fundamental behavior of the efficiency curve under various operating conditions. This set of experiments was performed at the baseline load of 3.5 bar NIMEP. All experiments were done at MBT spark timing. For each set of experiments the air-fuel ratio was set at stoichiometric conditions, and was then increased in increments of 0.2 lambda until the combustion process became unstable (COV of NIMEP>3). The lambda sweeps were repeated for three different compression ratios, three different enhancement levels (using both plasmatron and hydrogen enhancement), and EGR and air dilution. To study the effect of changes in air-fuel ratio at higher loads, a lambda sweep was also done at a load of 6.0 bar NIMEP and the baseline compression ratio of 9.8. The fuel used for these experiments was Indolene, Phillips Chevron UTG-96 [9], in order to make direct comparisons with past publications; Table 2 provides the fuel's properties.

Table 2 – Fuel properties of Phillips Chevron UTG-96

PROPERTY	
Research Octane Number	96.1
Motoring Octane Number	87.0
Lower Heating Value (MJ/kg)	43.1
Carbon Content (%)	86.5
Hydrogen Content (%)	13.5
Antiknock index	92
H/C molar ratio	1.93

The second set of experiments was used to develop efficiency correlations as a function of air-fuel ratio, compression ratio, and load. Neither reformate, nor hydrogen were used for this set of experiments. A three-point lambda sweep (λ = 1.0, λ = 1.3, λ = 1.6) at a constant baseline load of 4.0 bar NIMEP was performed to produce each curve. The load was selected to match as best as possible the operating conditions used in other publications, for comparison purposes. To study the effect of load and compression ratio on efficiency, lambda sweeps were performed at constant load, for three different loads, and the three compression ratios already mentioned. These experiments were performed with a fuel here termed "toliso," which is a mixture of 70% isooctane with 6.0 mL of TEL per gallon (PRF RON of 120) and 30% toluene. This mixture was selected because of its alkane/aromatic ratio, H/C ratio, energy content, and specific gravity, all similar to gasoline. The high octane number was needed to avoid knock at high loads and high compression ratios.

Reformate Addition

Using the same definitions and procedures as defined in [1, 3], a H_2, CO, N_2 mixture that a plasmatron fuel reformer would produce from a fraction of the gasoline, to enhance combustion was used for select data points. On a molar basis, the plasmatron mixture consisted of 25% H_2, 26% CO and 49% N_2. Up to four enhancement levels were applied: 0%, 15%, 30%, and 45% of the original gasoline flow.

Hydrogen Addition

Pure hydrogen was also use to speed up combustion, for a few points. The procedure used to inject hydrogen was similar to that of plasmatron gas. The hydrogen enhancement level was defined on an energy basis. Thus, 15% enhancement meant 15% of the total energy going into the engine was provided by hydrogen.

EGR measurements

The same procedure described in [3] was followed to apply and measure EGR; both the exhaust gases, and the EGR going into the intake manifold were sampled, using a Horiba emissions analyzer, and the CO_2 concentration was measured. The percent of EGR was then calculated as the ratio of the measured engine-in CO_2 to the measured engine-out CO_2.

RESULTS

COMBUSTION PHASING EFFECTS ON POWER

Tests were performed to determine the relationship between spark timing and engine output under a variety of conditions. Figure 1 shows the load vs. timing relationship for two different fuels at various air-fuel ratios. The differences across operating conditions are evident from the different timings at which the maximum torque occurs: as the air-fuel ratio increases, and the burning process becomes slower, the spark advance must be increased to obtain MBT timing; nevertheless the familiar torque shape that relates to the fundamental definition of MBT and one best spark timing is clear: as the timing is advanced or retarded from the optimum, torque is lost; during early combustion, work transfer from the piston to the gases near the end of compression is large, reducing the net work out of the engine; late combustion reduces the peak cylinder pressure, as well as the volume ratio and the temperature ratio through which the gases expand, decreasing the work output [2].

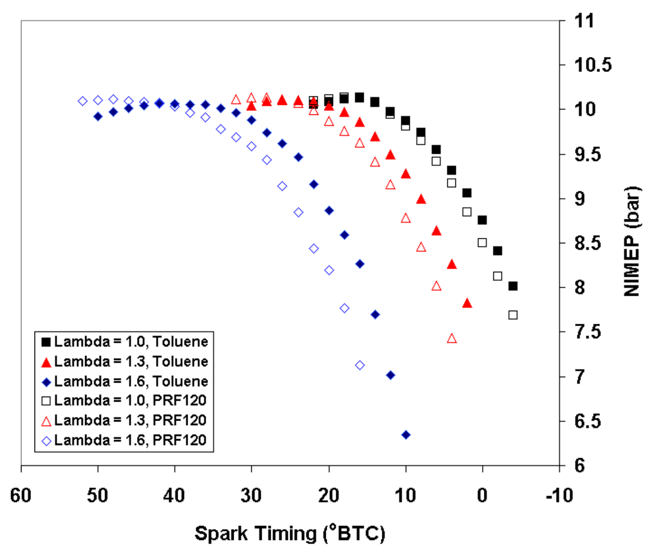

Fig. 1 – Effect of spark timing on NIMEP across range of air-fuel ratios; 1500 rpm, r_c = 9.8:1

If the NIMEP from the data in Fig. 1 is now normalized by the maximum NIMEP (at MBT timing), and if the spark timing is normalized by the MBT timing, the resulting plot is Fig. 2. The normalized spark timing, called "spark retard," is the spark timing in degrees ATC, minus the MBT spark timing. It represents the number of crank degrees that the spark timing has been shifted from optimum timing. This parameter allows for better understanding of combustion phasing. For example, the data shows that for a given spark retard, the faster burning points, i.e., the points with the latest absolute spark timing have the larger drop in NIMEP. The slower burning points have a slower drop in NIMEP. Alternatively, to get the same torque output, faster burning points require smaller spark retard than slower burning points.

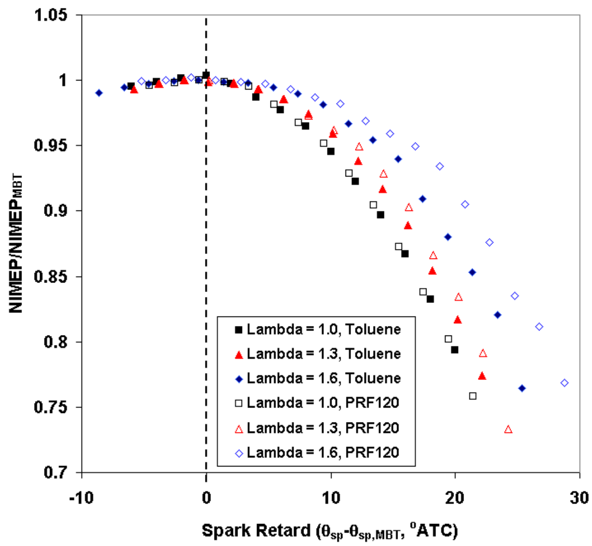

Fig. 2 – Effect of spark retard on normalized NIMEP across range of air-fuel ratios; 1500 rpm, r_c = 9.8:1

Figure 3 applies the same NIMEP and spark retard normalization across many different conditions, including different fuels, different air-fuel ratios, different compression ratios, different enhancement levels, and different intake pressures. The curve is well behaved, but there is some spread due to the different burning speeds.

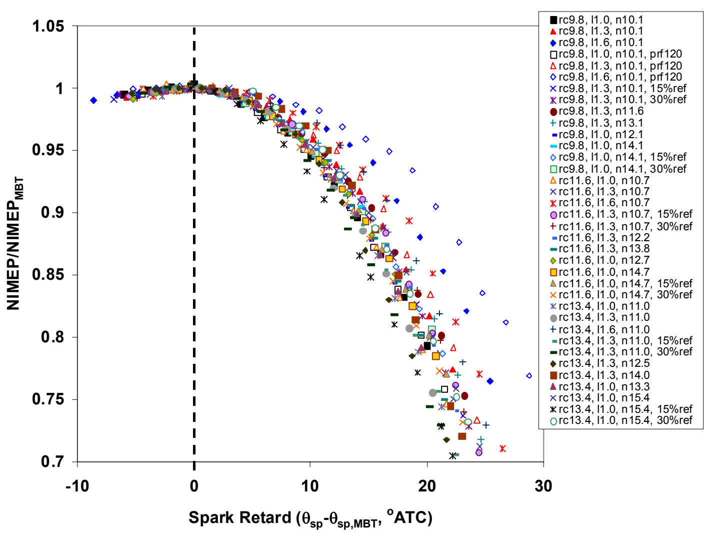

Fig. 3 – Effect of spark retard on normalized NIMEP across a wide range of operating conditions; 1500 rpm, r_c = 9.8:1, toluene fuel except where noted

A new combustion parameter was found that collapses all the data, across a wide variety of conditions, into one universal curve as shown in Fig. 4. This parameter termed "combustion retard" is defined as the location of 50% mass fraction burned, in degrees ATC, minus the location of 50% mass fraction burned at MBT spark timing. It represents the number of crank degrees that the center of the combustion event has been shifted from the timing for maximum torque. Figure 4 normalizes the same data shown in Fig. 3, using the new combustion retard parameter. The spread has been eliminated, and all the points fit well to a single curve. The equation of the curve fit is:

$$\frac{NIMEP}{NIMEP_{MBT}} = 1 - 0.168\left[\left(1 + 4.443 \cdot 10^{-3}\left(\theta_{50\%mfb} - \theta_{50\%mfb,MBT}\right)^2\right)^{0.5} - 1\right]$$

where $\theta_{50\%mfb}$ is the crank angle of 50% mass fraction burned in degrees ATC and $\theta_{50\%mfb,MBT}$ is the crank angle of 50% mass fraction burned at MBT spark timing. The quantity $\theta_{50\%mfb}$- $\theta_{50\%mfb,MBT}$ is the combustion retard.

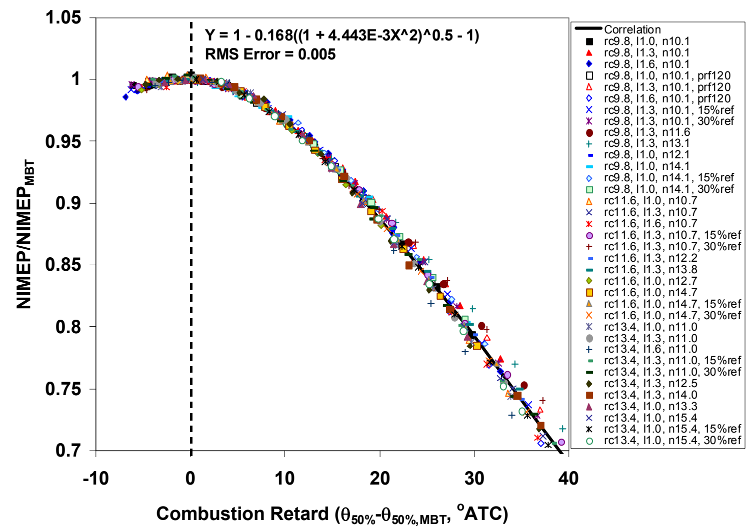

Fig. 4 – Effect of combustion retard on normalized NIMEP across a wide range of operating conditions; 1500 rpm, r_c = 9.8:1, toluene fuel except where noted

AIR-FUEL RATIO EFFECTS ON EFFICIENCY

Background

As the relative air-fuel ratio in an engine is varied, two regimes become apparent in the efficiency vs. lambda curve as seen in Fig. 5, and in previous literature [3, 4]. The first regime which starts at stoichiometric conditions and ends at the location of peak efficiency is characterized by a steadily increasing engine efficiency and a low variability in NIMEP. Following the location of peak efficiency begins the second regime which is characterized by a falling efficiency and a rapid increase in NIMEP variability. The practical lean drivability limit, defined as 2% of COV in NIMEP [8] is soon reached and is followed by a more erratic lean misfire limit. Figure 5 raises a few fundamental questions which have not yet been resolved: what determines the shape of the efficiency curve, what determines the location of both the peak efficiency and the drivability lean limit, and how can these be extended; what is the role of combustion variability; is there a direct link between the rapid fall in efficiency and the rapid rise in NIMEP variability?

Answers to these questions are important to get a better understanding of engine efficiency in general and more specifically, to improve lean and hydrogen-enhanced engine concepts.

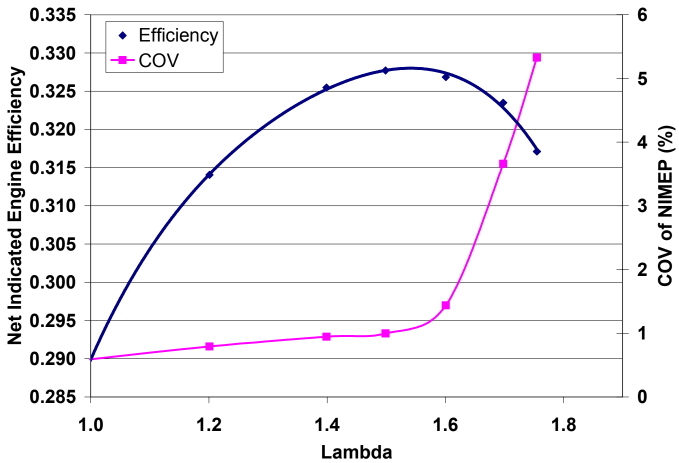

Fig. 5 – Effect of air-fuel ratio on efficiency and coefficient of variation in NIMEP; MBT timing, 1500 rpm, r_c = 9.8:1, NIMEP = 3.5 bar, Indolene

Methodology

To better understand these questions, combustion modeling was performed. MIT's engine cycle model was used to simulate the experimental results obtained in the test engine; details of this code can be found in [10]. The code was initially run at MBT conditions and a constant load of 3.5 bar NIMEP. The experimental burn durations were used as an input; these were generated using an in-house burn rate code. All other parameters such as engine geometry (e.g., compression ratio) and initial conditions were set to match the actual experimental setup.

Using the simulation, a framework was developed to analyze the effects of air-fuel ratio on efficiency. The framework consists of breaking down the changes in net indicated engine efficiency, relative to the baseline efficiency at stoichiometric conditions, into four different components: pumping losses, heat transfer losses, burn duration effects, and thermodynamic effects due to changes in the specific heat ratio, gamma. This method of analysis helps to understand the behavior of the efficiency curve, the location of the peak efficiency point, and the relative contribution of the variables affecting the efficiency.

Simulations were performed to isolate the effect of each variable, and thus determine the magnitude of its contribution to the overall efficiency. As a first step, a baseline efficiency was calculated for stochiometric conditions. The burn duration effect at each lambda was then calculated by running the code using each experimental burn duration and keeping all other variables constant at their baseline values. The new efficiency was then recorded. Similarly, the gamma or dilution effect was calculated by running the code at the baseline burn duration and heat transfer multiplier, while varying the air-fuel ratio. The pumping work was easily separated from each one of the runs, since it is provided as an output. To calculate the heat transfer effect, both the burn duration and the gamma simulations were run twice, first keeping the Woschni heat transfer model multiplier constant, and then holding the percent of energy loss due to heat transfer constant. The difference between the results from each pair of runs was determined to be the relative change in efficiency due to heat transfer changes. For higher loads, the Woschni heat transfer multiplier was reduced based on data shown in [2].

Simulation Results

Figure 6 shows the magnitude of the different efficiency components predicted by the simulation, and the resulting change in net indicated efficiency. The results are plotted as absolute differences, in percentage points, relative to the baseline efficiency which is set as the reference point. Thus for example, as the mixture gets leaner, and the burn duration gets longer, everything else being the same, the efficiency would fall by 1 percentage point at lambda of 1.5. From the graph one can observe the behavior of the three components that enhance efficiency. As the relative air-fuel ratio increases, the ratio of specific heats increases due to thermodynamic effects, contributing to higher efficiency through higher expansion work; the pumping losses decrease because the amount of throttling decreases and the intake pressure increases as a larger mass of air is inducted; the total heat transfer losses decrease as well, due to lower combustion temperatures at higher dilution levels. However, these positive efficiency contributions are countered by a lengthening burn duration which increases the time over which the energy is released, increasing the deviation from ideal conditions.

The actual data is also shown in this chart. The agreement between the changes in the simulated total efficiency and the actual data is excellent. One discrepancy, not shown here, is that the absolute magnitude of the MIT model efficiency is 10% higher than the data. This difference can be accounted by the in-cylinder combustion inefficiency, which is not included in the model [11, 2]. Nevertheless the relative change between each point in the data is correctly predicted by the model.

It is important to note that the simulated peak efficiency location matches the actual location of peak efficiency, indicating that the detrimental impact due to lengthening burn duration has been well captured. From the graph it is clear that the eventual decrease in efficiency is due to the increasingly negative impact of the lengthening burn duration.

The agreement for different loads and different compression ratios was also quite good, as will be seen in later sections. This shows that the magnitude of each efficiency component has been adequately represented, and that this framework explains the shape of this efficiency curve.

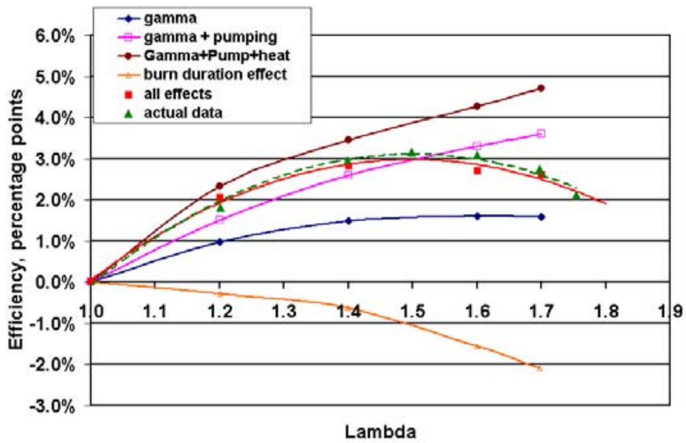

Fig. 6 – Air-fuel ratio effect on efficiency, comparison of simulation results and actual data; MBT timing, 1500 rpm, r_c = 9.8:1, NIMEP = 3.5 bar, Indolene

Effect of 10-90% burn duration

As already seen, the time it takes to burn the mass in the cylinder has a major impact on the overall net indicated efficiency. In particular, the length of the time between burning 10% of the mass and 90% of the mass, also known as the 10-90% burn duration and commonly associated with the flame propagation stage, is the most relevant for efficiency. Some references [6] agree with this statement, but this conclusion can be drawn from the data presented in this section.

In Fig. 7, combustion has been speeded up using different levels of hydrogen enhancement (as a percent of total energy into the engine) at the same constant load of 3.5 bar NIMEP. The result is a downward shift in the overall 10-90% burn duration curve (faster combustion), and an increase in net indicated efficiency with higher enhancement levels, relative to pure indolene. This graph shows that the burn duration at which the peak efficiency occurs, is constant, at approximately 30 CAD, irrespective of any shifting of the 10-90% burn duration curve. Connecting this observation to Fig. 6, two main implications emerge. The effect of the entire burn duration process (0-100%) on efficiency is dominated by the 10-90% burn duration. Thus the burn duration effect shown in Fig. 6, can be thought of as the 10-90% burn duration effect. The second important implication is that there exists a critical 10-90% burn duration beyond which the detrimental effect on efficiency increases rapidly. Consequently, because of the balance of effects shown in Fig. 6, peak efficiency will occur right before this large increase in negative impact, or approximately at 30 CAD, for this specific engine. The deteriorating effect on efficiency caused by slower combustion can no longer be made up by the other positive factors such as pumping work reduction, heat transfer reduction, and thermodynamic effects.

The conclusion that the 10-90% is the dominating combustion component on the engine efficiency is not surprising because 80% of the total fuel is burned during this interval. However, what is surprising is that there is a limiting burn duration (30 CAD) beyond which the detrimental effect on efficiency increases substantially, causing the efficiency curve to bend downwards. This effect is not fortuitous, as it was observed across a variety of conditions. Figure 8 also shows the limiting 30 CAD while comparing different compression ratios at the same 3.5 bar NIMEP load. Similarly, Fig. 9 shows the same point using EGR dilution. At higher loads (Fig. 10), and different turbulence levels (Fig. 11), created using different turbulence plates [1,4], the limiting burn duration was also 30 or 29 CAD, the difference of 1 CA degree being within experimental error.

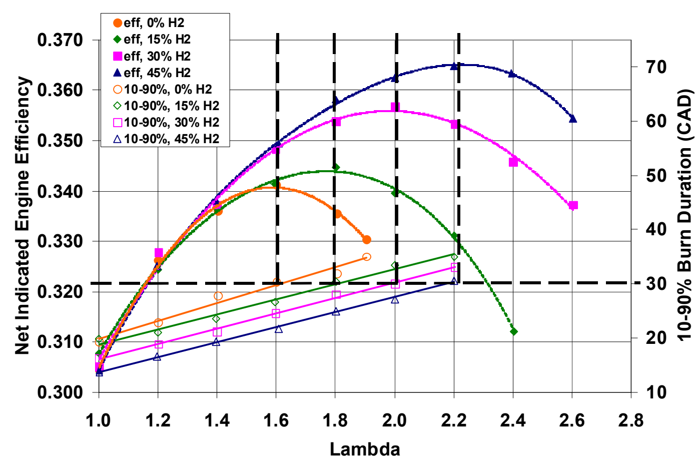

Fig. 7 – Air-fuel ratio effect on efficiency and burn duration for different levels of hydrogen enhancement; MBT timing, 1500 RPM, r_c=13.4:1, NIMEP = 3.5 bar, Indolene

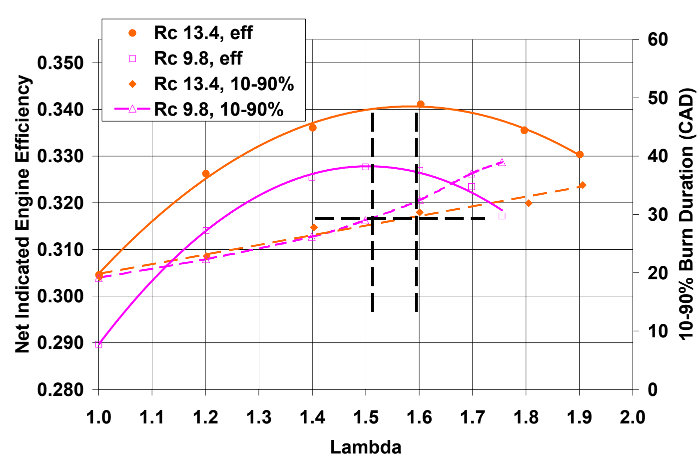

Fig. 8 – Comparison of air-fuel ratio effect on efficiency and burn duration for two different compression ratios; MBT timing, 1500 RPM, NIMEP = 3.5 bar, Indolene

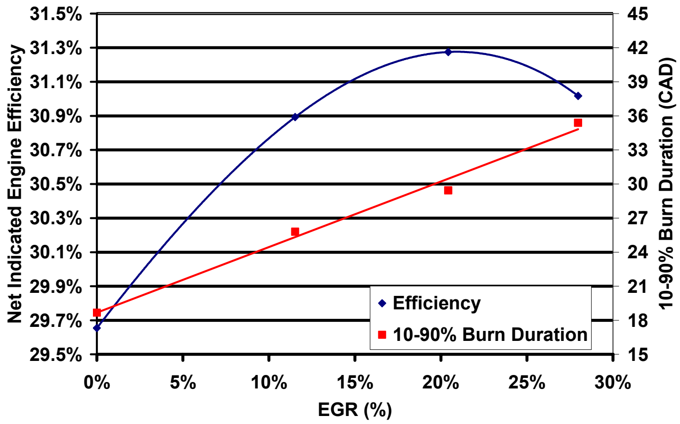

Fig. 9 – EGR effect on efficiency and burn duration; MBT timing, 1500 RPM, r_c=9.8:1, NIMEP = 3.5 bar, Indolene

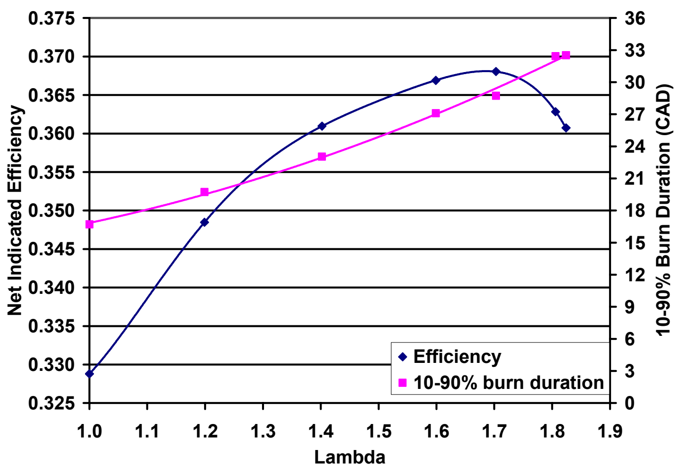

Fig. 10 – Air-fuel ratio effect on efficiency and burn duration at high load; MBT timing, 1500 RPM, r_c=9.8:1, NIMEP = 6.0 bar, Indolene

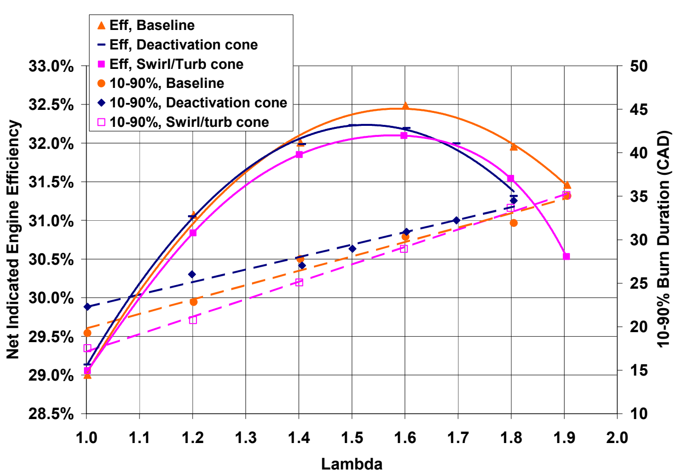

Fig. 11 – Air-fuel ratio effect on efficiency and burn duration for different turbulence cones; MBT timing, 1500 RPM, r_c=9.8:1, NIMEP = 3.5 bar, Indolene

To obtain more insight behind the limiting 10-90% burn duration, laminar flame speed calculations were done; the hypothesis was that if a limiting burn duration indeed exists, then keeping the level of turbulence constant, the laminar flame speed at peak efficiency should be the same across a range of conditions. This assumes that the speed of flame propagation is composed of a laminar and a turbulent component. The conditions at the location of peak efficiency for the different curves shown in Fig. 7 were replicated. The temperature and pressure were approximated through an isentropic compression of the unburned gas, and using the necessary engine geometry at the specified location. For all three types of hydrogen enhancement the temperature and pressure were all close to 830 K and 30 atm, respectively. Using CHEMKIN, methane was used as the fuel, due to its reliable, and well established, mechanism. Figure 12 shows the laminar flame speed curves for methane, at the three levels of hydrogen enhancement. The location of peak efficiency is also noted. It stands out that the laminar flame speed at the location of peak efficiency for each level of enhancement is constant, close to 50 cm/sec. This reinforces the conclusion that there is a limiting duration for burning the 10-90% mass fraction.

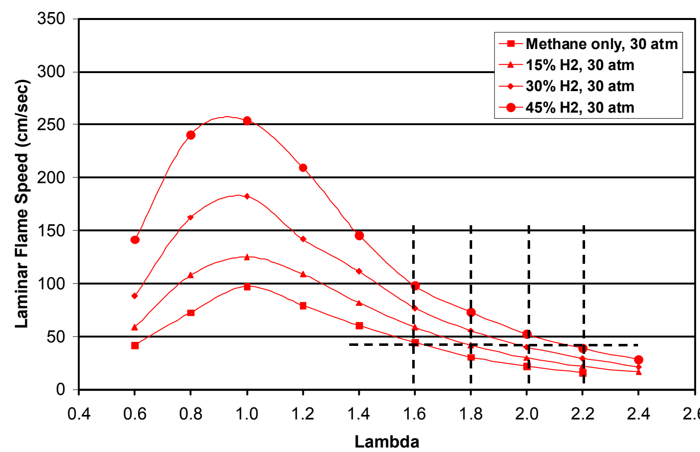

Fig. 12 – Air-fuel ratio effect on laminar flame speed for different levels of hydrogen enhancement with CH_4 as the fuel; 830 K, 30 atm

Effect of 0-10% burn duration

Thus far, we have concluded that the 10-90% burn duration is the main variable controlling efficiency. Consequently, the variability in 10-90% burn duration will cause variability in NIMEP. Figure 13 shows the close link between the variability in these two variables. This chart shows the ratio of the actual standard deviation to the baseline stoichiometric standard deviation for NIMEP, 10-90% burn duration, and 0-10% burn duration. As the relative air-fuel ratio is varied, the variability in NIMEP follows the same trend as the variability in the 10-90% burn duration; the variability for both cases starts low, and quickly surpasses the initial stoichiometric variability by a factor greater than 2 beyond lambda of 1.4. The variability in the 0-10% burn duration however stays fairly low and remains well behaved, closer to the baseline stoichiometric variability. It does have a more rapid increase at the lean limit (λ=1.7), but the overall behavior of this curve does not coincide with the variability of the NIMEP or the variability of the 10-90% burn duration. Additionally, the extensive data produced for this paper, does not show a clear link between the 0-10% burn duration variability (plotted as standard deviation), and the standard deviation of the 10-90% burn duration (or alternatively the COV of NIMEP), as other publications have stated [6, 7]. However, the data does show that the 0-10% burn duration itself seems to control the variability in the 10-90% burn duration, and consequently the variability in NIMEP (Fig. 13, 14). More specifically, there is a limiting 0-10% burn duration, rather than a limiting variability, at which combustion becomes erratic irrespective of enhancement level, type of dilution, compression ratio, or load. Figure 14 shows that at 40 CAD the COV of NIMEP is close to 2% for all conditions tested. This value of COV was chosen because the data is still well behaved, not having yet reached the lean misfire limit, and because it is typically used in industry as the practical COV drivability limit [8]. Figure 15 shows a similar limiting behavior when the COV in NIMEP is plotted against the 10-90% burn duration. The authors believe that the first combustion event, 0-10% burn duration, is the cause for the similar behavior of the second combustion event, 10-90% burn duration. Figure 16 shows a specific comparison between different compression ratios, where the limiting flame initiation duration of 40 CAD is clear.

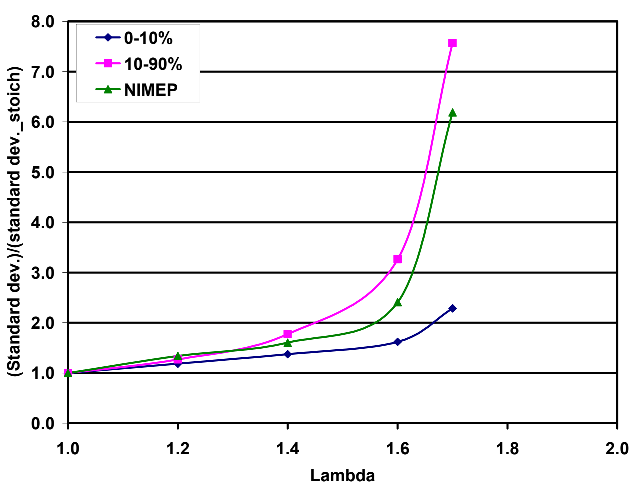

Fig. 13 – Variability of NIMEP, 10-90% burn duration, and 0-10% burn duration with air-fuel ratio; MBT timing, 1500 RPM, r_c=9.8:1, NIMEP = 3.5 bar, Indolene

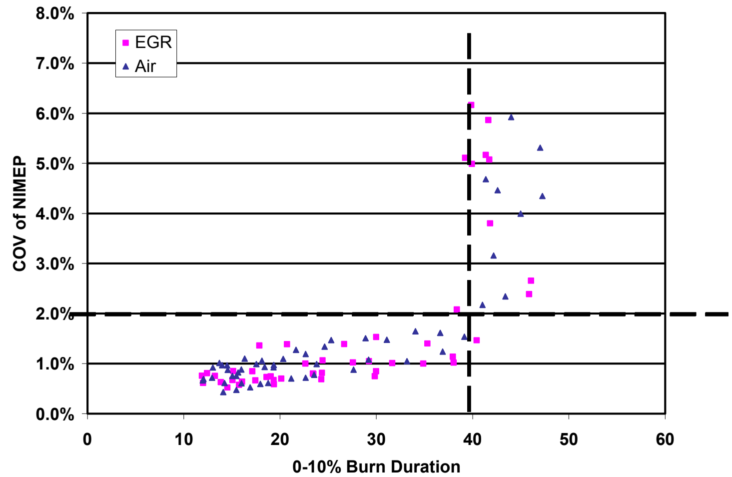

Fig. 14 – Changes in COV of NIMEP with 0-10% burn duration; MBT timing, 1500 RPM, r_c=9.8:1, NIMEP = 3.5 bar, Indolene

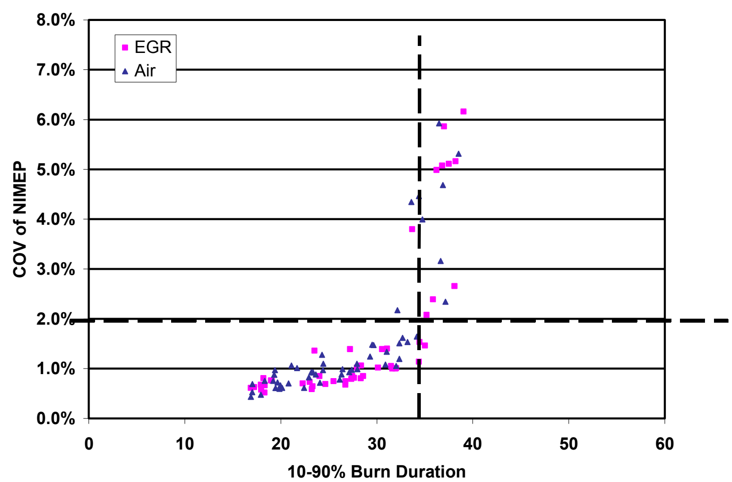

Fig. 15 – Changes in COV of NIMEP with 10-90% burn duration; MBT timing, 1500 RPM, r_c=9.8:1, NIMEP = 3.5 bar, Indolene

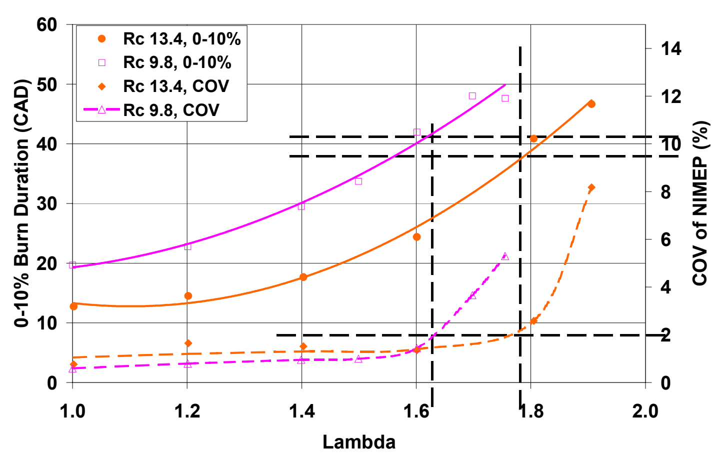

Fig. 16 – Relationship between coefficient of variation and 0-10% burn duration as air-fuel ratio increases for two different compression ratios; MBT timing, 1500 RPM, r_c=9.8:1, NIMEP = 3.5 bar, Indolene

Location of Peak Efficiency Relative to Combustion Instability

In past publications, with experiments done at lower compression ratios [1, 4] it was thought that the peak in net indicated efficiency and the onset of combustion instability, as indicated by the rapid rise in COV of NIMEP, were directly linked. The curves typically lined up at peak efficiency and the onset of variability. However, this was not the case for the higher compression ratios used during this research. To examine this issue, one must again look at the burn durations for answers.

Figure 17 shows the non-linear relationship between the 10-90% burn duration and the 0-10% burn duration. Initially, the length of the 0-10% burn duration changes at a lower rate than the 10-90% burn duration (higher initial slope); but moving further along the x-axis, as the 0-10% burn durations get longer, the 10-90% burn duration increases at a lower rate, thus the slope at the longer burn duration end of the curve is lower than the slope at the beginning, or the faster burn duration part of the curve. This can be explained because at the higher burn durations, where the level of dilution is higher, the laminar flame speed, which strongly affects the 0-10% burn duration is lower, but the level of turbulence, which primarily dominates the 10-90% burn duration remains about the same. Thus, due to its weaker laminar flame speed dependence, the 10-90% burn duration will see less of a lengthening effect at higher dilution (higher burn durations), than the 0-10% burn duration.

The figure also shows the same trend for a higher compression ratio and for 30% plasmatron enhancement. The initial offset of the high compression ratio curve relative to the lower compression ratio curve can also be explained. For a given 10-90% burn duration, the flame initiation stage is faster for the higher compression ratio due to the higher laminar flame speeds caused by the higher pre-combustion temperatures, and due to a lower residual fraction. This faster laminar flame speed has the most impact on the 0-10% burn duration. Similarly, a faster laminar flame speed due to hydrogen addition explains the offset of the 30% enhancement curve.

Figure 18 shows the burn duration relationship for all data at various compression ratios, various plasmatron enhancement levels, air dilution, and EGR dilution, at MBT spark timing, and 3.5 bar NIMEP load. This figure shows that the 10-90% burn duration vs. 0-10% burn duration curve keeps the same shape irrespective of operating conditions. However, and as discussed previously, the exact relationship between the burn durations changes at different operating conditions, as witnessed by the vertical spread in the data, due to the differences in laminar flame speeds.

Using the two previous conclusions, that is, the fixed relationship between 10-90% burn duration and efficiency, and the fixed relationship between 0-10% burn duration and 10-90% burn duration variability (or NIMEP variability), and knowing that the relationship between the 10-90% and 0-10% burn duration changes (at least until 2% COV of NIMEP is reached), as shown in Figs. 17 and 18, it follows that the location of peak efficiency and combustion instability will change relative to each other. Figure 19 shows this observation at two different compression ratios. For the high compression ratio, the onset of combustion instability occurs further away from the location of peak efficiency than in the lower compression ratio case. The implication of this is that the peak in net indicated engine efficiency and the rapid rise in combustion instability are not directly linked (at least not necessarily), and they happen at different locations depending on the operating conditions. Another implication, as will be examined more closely in the next section, is that variability only becomes important at or after the location of peak efficiency.

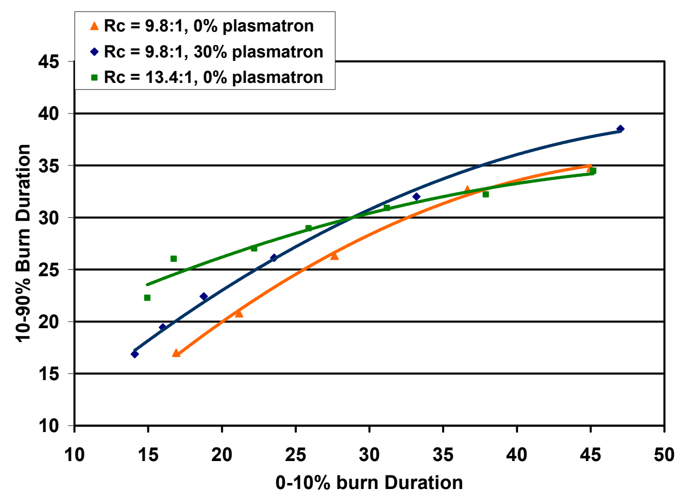

Fig. 17 – Relationship between 10-90% burn duration and 0-10% burn duration for different levels of plasmatron enhancement; MBT timing, 1500 RPM, r_c=9.8:1, NIMEP = 3.5 bar, Indolene

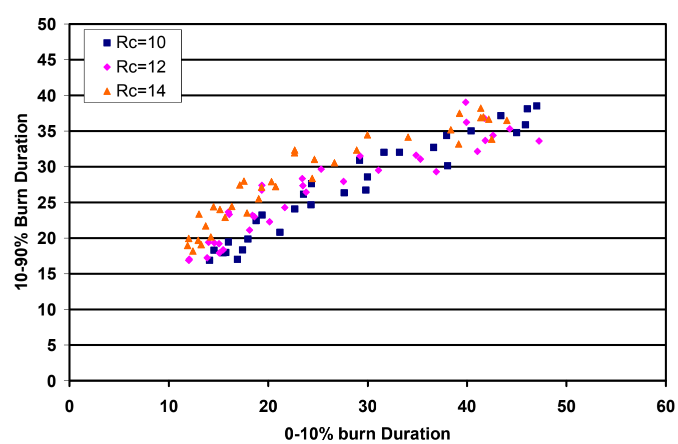

Fig. 18 – Relationship between 10-90% burn duration and 0-10% burn duration for three different compression ratios using three levels of plasmatron enhancement; MBT timing, 1500 RPM, NIMEP = 3.5 bar, Indolene

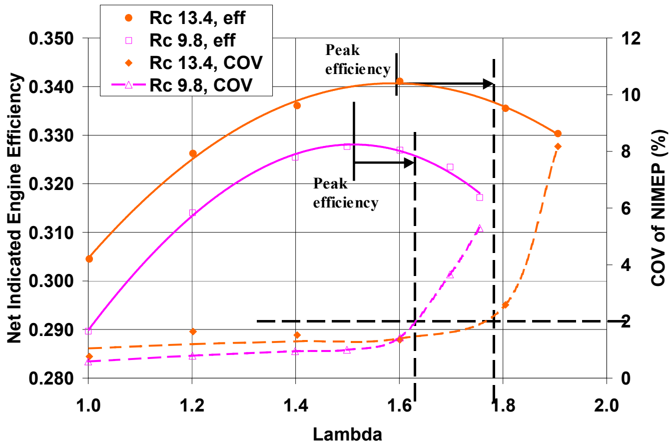

Fig. 19 – Relationship between efficiency and coefficient of variation with increasing air-fuel ratio for two different compression ratios; MBT timing, 1500 RPM, NIMEP = 3.5 bar, Indolene

Effect of Combustion Variability on Efficiency

To understand the effect of combustion variability on efficiency, as the air-fuel ratio increases, it is necessary to look at the distribution of the individual cycles that compose each data point. Figures 20 and 21 lay out both the NIMEP and the 10-90% burn duration distributions, respectively, for the 300 cycles that make up each point in Fig. 5. An appropriate probability density function, that can accurately describe each data set, has also been superimposed to the data, as shown. Note the similarity between the NIMEP and the 10-90% burn duration distributions at each value of lambda, an expected observation based on the previous discussion on the effects of the 10-90% burn duration.

Although variability, as defined by the standard deviation of the mean for each data set, steadily increases relative to baseline stoichiometric conditions, it only becomes significant after the location of peak efficiency, around λ=1.6. Before this point is reached, variability does not affect efficiency. This occurs because even though the spread among the distribution keeps increasing, the data stays symmetrical and does not affect the average of either the NIMEP or the 10-90% burn duration. This can be verified by looking at the good agreement between the data and the superimposed Gaussian curves. Because of this symmetry, any cycles with low NIMEP are canceled out by cycles with high NIMEP. Consequently, any reduction in the spread, or variability, in the NIMEP distribution before the peak efficiency point, will not shift the average NIMEP, and thus will not affect the efficiency. However, beyond the peak efficiency point, the spread not only keeps increasing, but the data distribution also takes an asymmetrical shape which can be described using a Gamma distribution as shown. The effect of variability on efficiency is now important since this asymmetric distribution has effectively shifted the average NIMEP and the average 10-90% burn duration, from what would have been obtained had the data kept a normal (i.e., Gaussian) shape. In other words, any reduction in the spread of the data with these asymmetrical distributions will now shift the overall average of the data, increasing the NIMEP average and thus the efficiency.

Knowing that when the data behaves symmetrically it does not affect efficiency, it is possible to use the normal distribution as an upper limit to quantify the effect of combustion variability on the net indicated efficiency. Figure 22 shows the resulting shift in the average NIMEP when a Gaussian distribution is superimposed on that part of the data that most closely resembles a symmetric distribution. The result is a shift in the NIMEP average, increasing the net indicated efficiency. The average 10-90% burn duration distribution that results when only the NIMEP data enclosed by the superimposed Gaussian distribution from Fig. 22 is considered is also shown in Fig. 23. The average of the 10-90% burn duration has also shifted, becoming faster. This is consistent with the previous discussions of how the 10-90% burn duration and NIMEP go hand-in-hand, and how at MBT timing conditions a faster 10-90% burn duration is preferred and will have a lesser negative impact on the overall efficiency. Figure 24 shows the resulting efficiency and 10-90% burn duration curves assuming a normal distribution for all the data. In essence, variability does not play a role in these new curves, however, the efficiency still falls due to the lengthening burn duration. The original efficiency and burn duration curves are also shown in this graph. Comparing both efficiency curves, one can see that the efficiency loss due to variability is modest, around 2%.

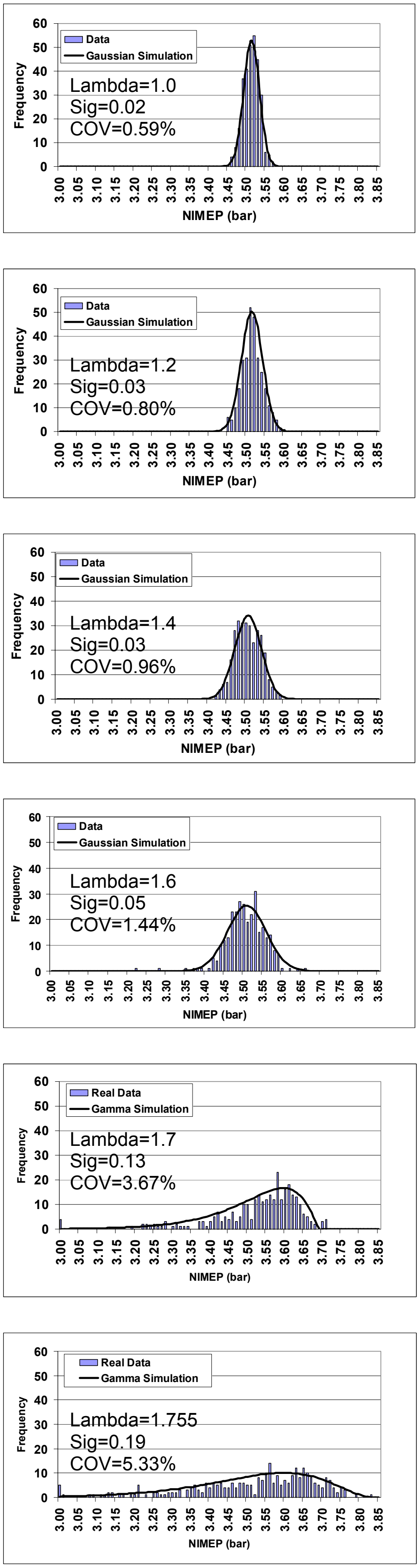

Fig. 20 – NIMEP distribution for different air-fuel ratios; MBT timing, 1500 RPM, r_c=9.8:1, NIMEP = 3.5 bar, Indolene

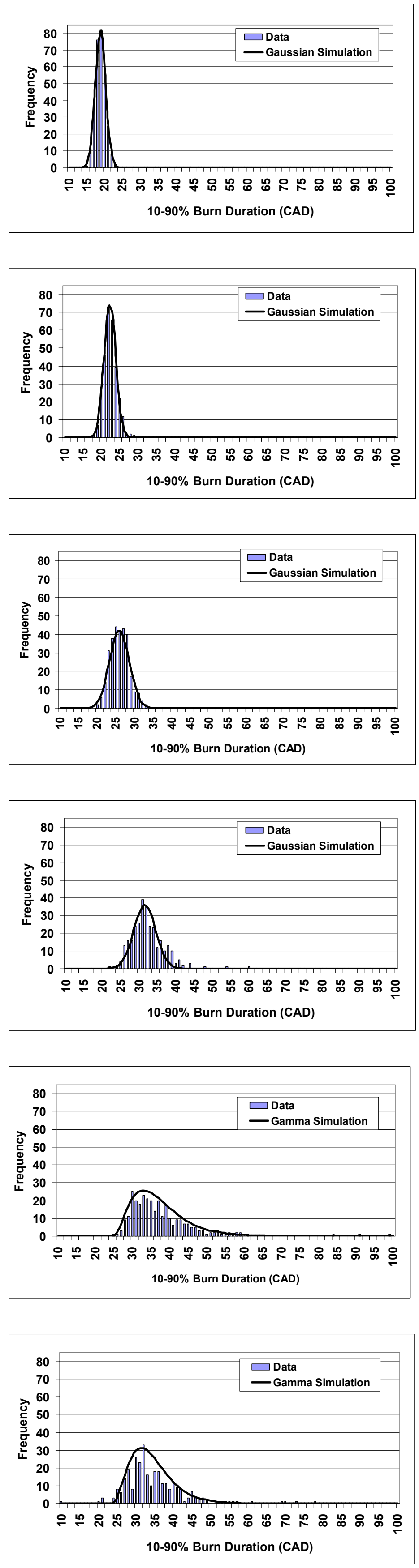

Fig. 21 – 10-90% burn duration distribution for different air-fuel ratios; MBT timing, 1500 RPM, r_c=9.8:1, NIMEP = 3.5 bar, Indolene

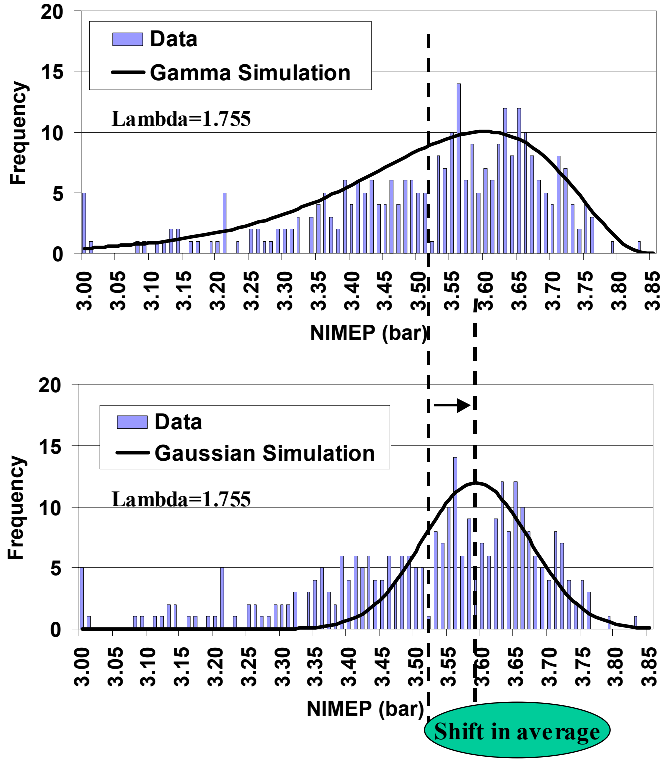

Fig. 22 – Comparison between symmetric and asymmetric NIMEP distributions, and their effect on the overall average; MBT timing, 1500 RPM, r_c=9.8:1, NIMEP = 3.5 bar, Indolene

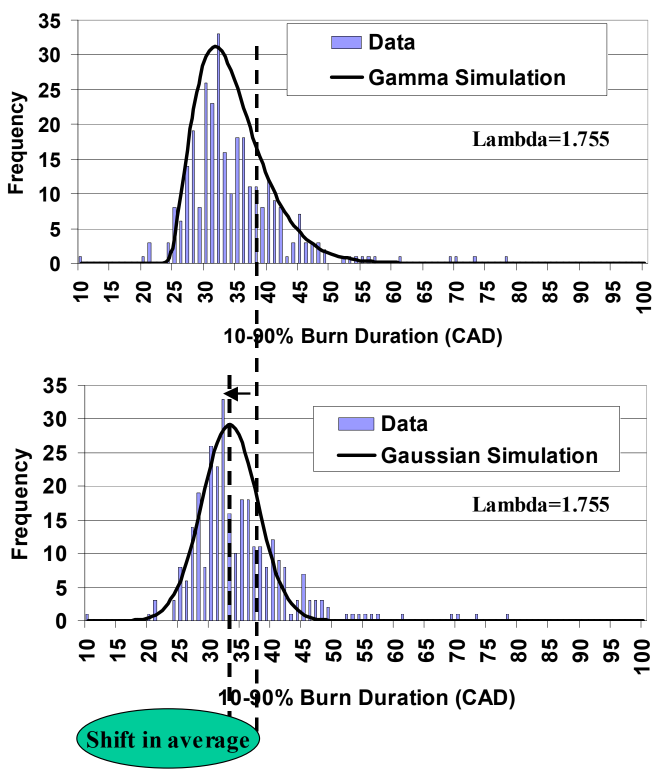

Fig. 23 – Comparison between symmetric and asymmetric 10-90% burn duration distributions, and their effect on the overall average; MBT timing, 1500 RPM, r_c=9.8:1, NIMEP = 3.5 bar, Indolene

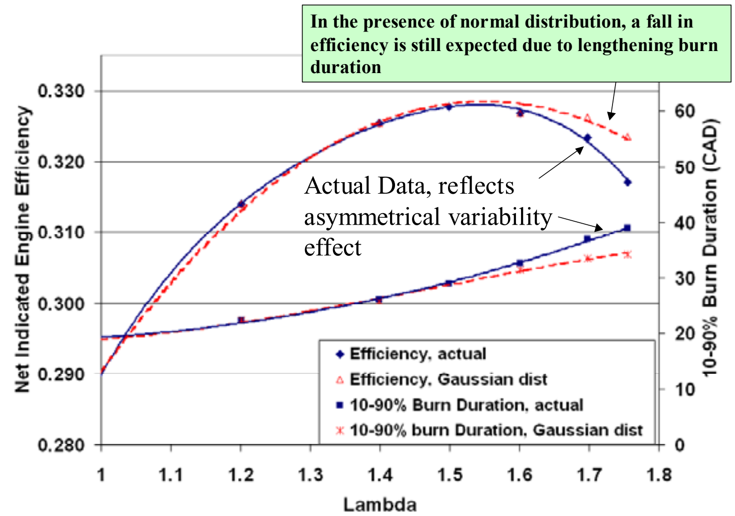

Fig. 24 – Effect of asymmetric NIMEP and burn duration distributions on efficiency; MBT timing, 1500 RPM, r_c=9.8:1, NIMEP = 3.5 bar, Indolene

COMPRESSION RATIO EFFECTS ON EFFICIENCY

The impact of higher compression ratio on the baseline efficiency at stoichiometric conditions is seen in Fig. 25. This figure shows the absolute efficiencies, starting from the estimated ideal gross indicated efficiency for a compression ratio of 9.8:1, as well as the breakdown of the efficiency changes that lead to the net indicated efficiency for a compression ratio of 13.4:1. The changes in efficiency have been separated into heat transfer effect, pumping losses, expansion work, and burn duration effect. The absolute pumping loss has increased at the higher compression ratio. Higher efficiency has required a higher throttling (less air and less fuel), to maintain a load of 3.5 bar NIMEP. The absolute heat transfer has also increased at the higher compression ratio due primarily to higher temperatures and an increase in the surface area to volume ratio [2, 5] but the overall percentage of the total efficiency is lower. The small differences in burn duration at stoichiometric conditions (Fig. 31) do not contribute to any differences in the baseline efficiencies, and so, this effect has been neglected. However, as the air-fuel ratio increases, the 10-90% burn duration for the higher compression ratio becomes shorter than the burn duration for the 9.8:1 compression ratio, as shown in Fig. 31, and consequently, the detrimental effect due to burn duration also becomes smaller for a given lambda. The majority of the efficiency increase is due to the thermodynamic effect of having a larger volume expansion ratio.

The same framework used to explain the efficiency behavior with air-fuel ratio in the previous section can also be used to explain the efficiency behavior for higher compression ratios as the air-fuel ratio changes. Figure 26 shows the simulation results for a compression ratio of 13.4:1. The match between the simulation and the data is good, and the predicted location of peak efficiency is also accurate. The first thing to notice from this chart is the extension of the peak efficiency point, relative to a compression ratio of 9.8:1 (Fig. 6). This extension of almost 0.1 lambda results from a faster 10-90% burn duration, which shifts the λ-value at which the critical burn duration of 30 CAD occurs.

The relative magnitude of the efficiency components has also changed relative to the lower compression ratio, as shown in Fig. 27. The two components that show the largest relative difference between compression ratios, as the air-fuel ratio increases, are burn duration and gamma. As expected, the relative effect of burn duration at the higher compression ratio is lower with higher lambda than at the lower compression ratio, due to the faster 10-90% burn duration at the high compression ratio, and due to the higher efficiency impact from other components. For high compression ratio, the effect of gamma on efficiency, relative to stoichiometric conditions, has decreased compared to the lower compression ratio.

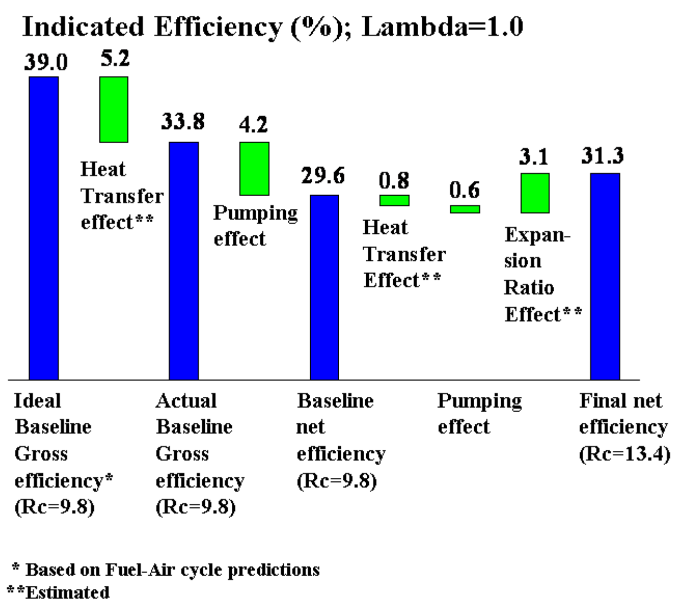

Fig. 25 – Comparison of efficiency change between two different compression ratios; MBT timing, 1500 RPM, NIMEP = 3.5 bar, Indolene

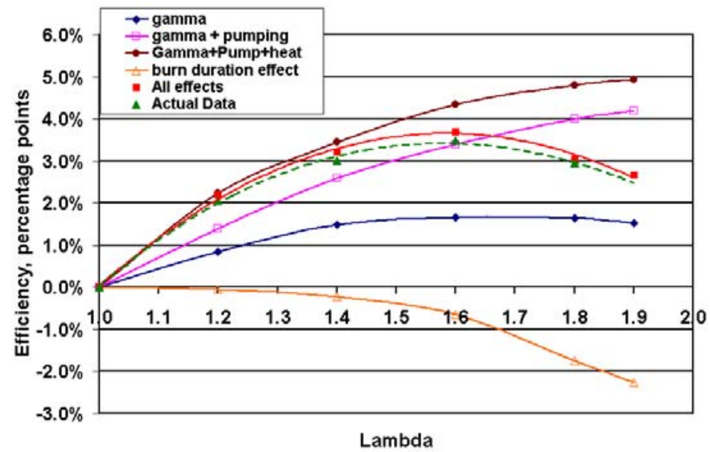

Fig. 26 – Air-fuel ratio effect on efficiency, comparison of simulation results and actual data; MBT timing, 1500 rpm, r_c = 13.4:1, NIMEP = 3.5 bar, indolene

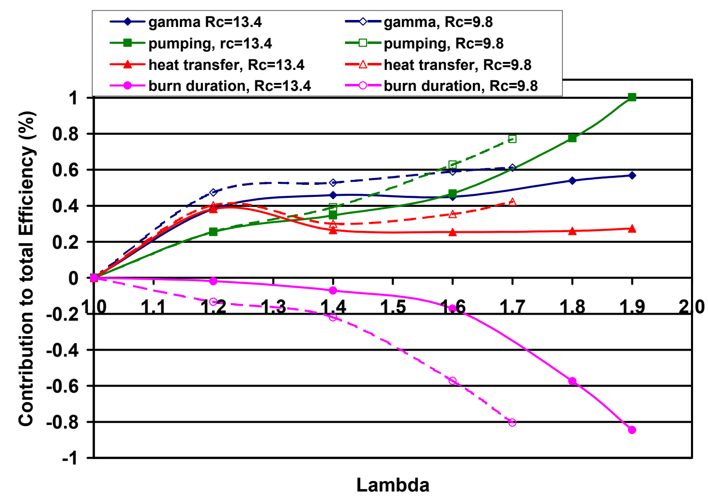

Fig. 27 – Comparison of relative efficiency contributions between two different compression ratios; MBT timing, 1500 RPM, NIMEP = 3.5 bar, Indolene

LOAD EFFECTS ON EFFICIENCY

As the load increases, the efficiency also increases due primarily to reduced pumping losses, as more air is inducted into the combustion chamber, and due to reduced heat transfer as a percent of the total fuel consumed. Figure 28 shows the source and approximate magnitude of the total efficiency increase at 6.0 bar NIMEP and stoichiometric conditions, relative to a baseline load of 3.5 bar NIMEP at the same air-fuel ratio. A reduction in pumping loss dominates the change in efficiency, accounting for approximately 80% of the net indicated efficiency increase. The remaining 20% of the efficiency increase is associated with reduced heat transfer. Although the 10-90% burn duration at the high load is overall faster, as shown in Fig. 31, due to reduced residual and higher combustion temperatures, previous experiments at the Sloan lab have shown that under stoichioimetric conditions a reduction in 4 CAD on the 10-90% burn duration has a small effect on efficiency. This is verified in Fig. 7, where faster burn durations caused by hydrogen enhancement at stoichiometric conditions show small changes in efficiency (less than 0.3%). Thus, the effect of burn duration on efficiency for this stoichiometric case, has been assumed to be zero. Nevertheless, when the air-fuel ratio is increased, burn duration once again is critical in determining the overall efficiency, as shown in Fig. 29. This chart shows the behavior of the actual efficiency and the simulated efficiency with changes in air-fuel ratio at the higher load. The agreement between the simulation and the data is good. The simulation does not predict the initial efficiency slope very accurately, but does an excellent job at predicting the relative efficiency changes between the rest of the points, as well as the location of the peak efficiency. This last one is located at lambda of 1.7, representing an extension of 0.2 lambdas relative to the baseline load (3.5 bar NIMEP).

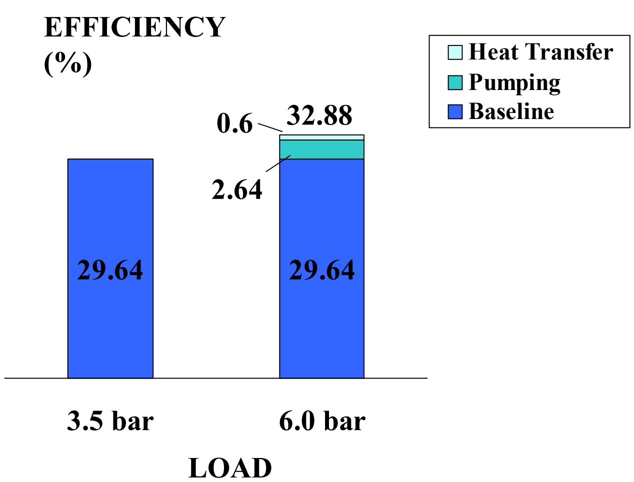

Fig. 28 – Comparison of changes in net indicated efficiency between two different loads; MBT timing, 1500 RPM, r_c=9.8:1, Indolene

Figure 30 shows the relative effects of each simulated efficiency component with increasing air-fuel ratio, for both 3.5 bar NIMEP and 6.0 bar NIMEP. One can notice the reduced effects from burn duration, and heat transfer at the higher load. Pumping work also shows a lower effect at the high load, since the reference point of comparison is the stoichiometric efficiency, where pumping losses are already much lower than at the lower load. Gamma is not affected significantly with load but because the relative effect of the other efficiency components has decreased, the relative impact of gamma is now slightly higher at the higher load, than at the lower load.

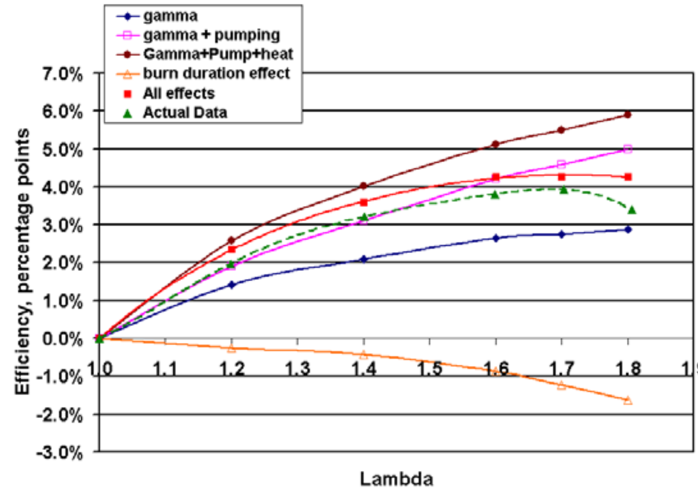

Fig. 29 – Air-fuel ratio effect on efficiency, comparison of simulation results and actual data; MBT timing, 1500 RPM, r_c = 9.8:1, NIMEP = 6.0 bar, Indolene

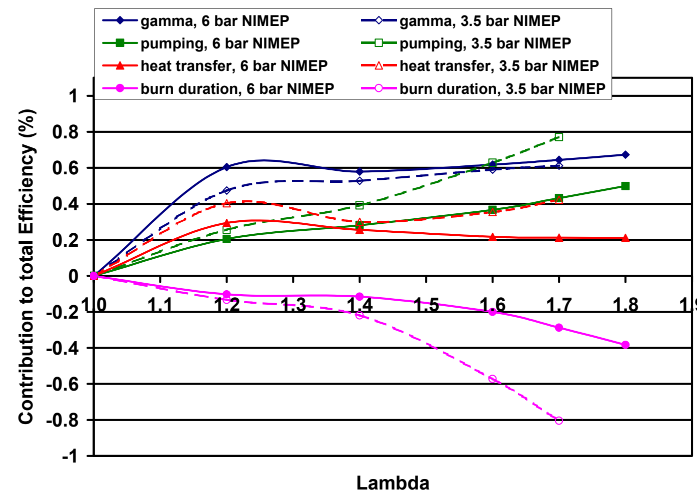

Fig. 30 – Comparison of relative efficiency contributions between two different loads; MBT timing, 1500 RPM, r_c = 9.8:1, NIMEP = 3.5 bar, Indolene

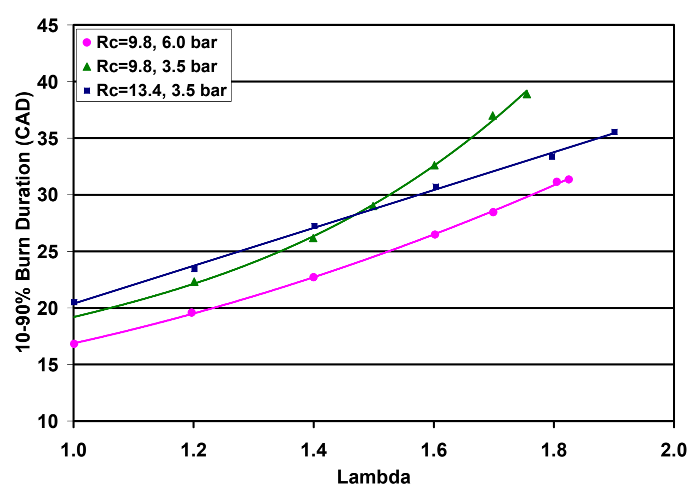

Fig. 31 – Comparison of changes in burn duration with increasing air-fuel ratio for different loads and compression ratios; MBT timing, 1500 RPM

EFFICIENCY CORRELATIONS

The following charts provide useful well-behaved correlations that summarize the effect of load, air-fuel ratio, and compression ratio on efficiency, at two different speeds. The trends agree with the explanations provided in the previous sections

The improvement of efficiency with air-fuel ratio, relative to stoichiometric conditions, across three different compression ratios is shown in Fig. 32. Higher compression ratio extends the location of peak efficiency, due to faster burn durations, as previously described. The relative improvement in efficiency decreases as the compression ratio increases, in spite of higher absolute changes, due to higher baseline indicated efficiencies with higher compression ratios, as shown in Fig. 25.

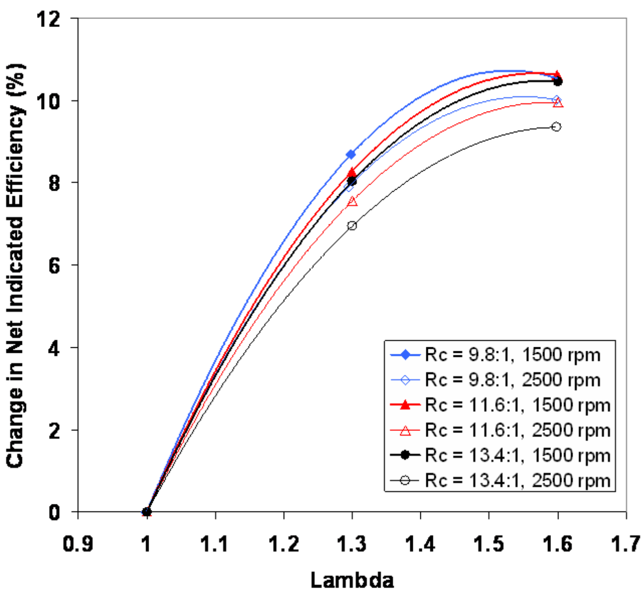

Fig. 32 - Normalized change of net indicated efficiency with lambda; Load = 4.0 bar NIMEP

Changes in net indicated efficiency with load are shown in Figs. 33 and 34, for different compression ratios at two different speeds. The efficiency improvements are relative to baseline mid-load of 4.0 bar NIMEP. Relative to this reference point, efficiency improves by about 6% per bar NIMEP. The curves are well aligned, but the higher compression ratio curves are steeper, most likely due to differences in throttling effects and heat transfer with compression ratio. As previously explained, to maintain constant load, the amount of throttling must be increased with higher compression ratio, due to the higher efficiencies obtained. Consequently, the relative impact from reduced pumping losses as the load increases will be higher for the more throttled, higher compression ratio. There will be a similar effect due to reduced heat transfer. The same trend is observed for leaner conditions, as shown in Fig. 34. The overall efficiency improvement under lean conditions is less than at stoichiometric conditions because baseline efficiencies are higher due to reduced pumping losses with higher manifold air pressures.

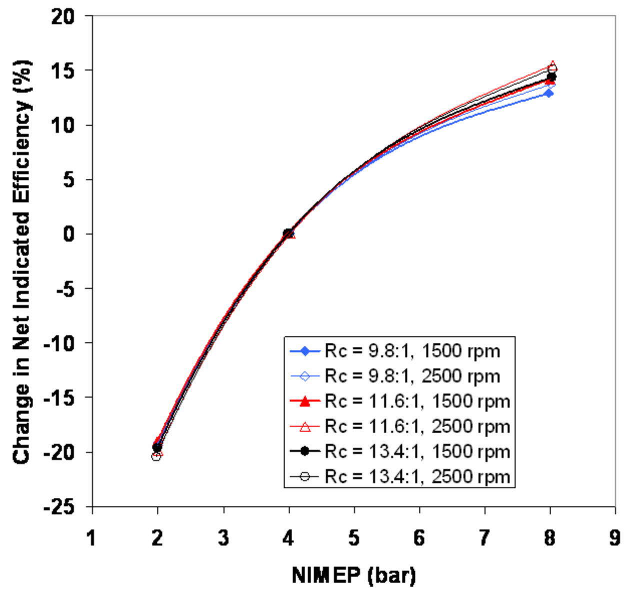

Fig. 33 - Normalized change of net indicated efficiency with NIMEP; Lambda =1.0

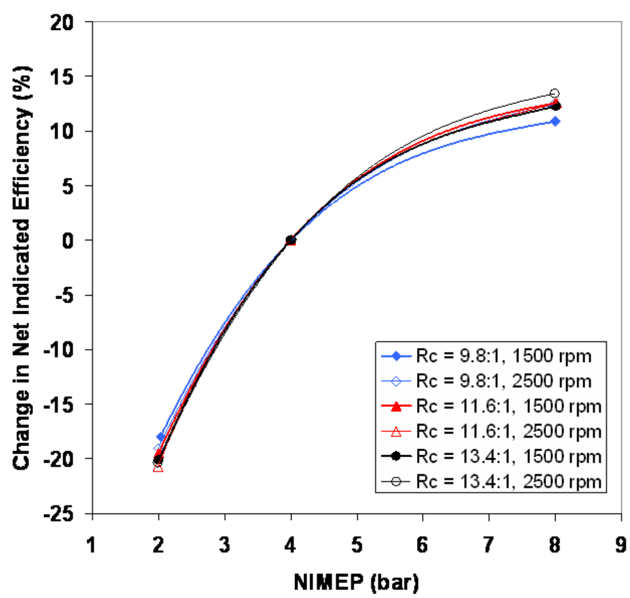

Fig. 34 - Normalized change of net indicated efficiency with NIMEP; Lambda =1.3

The effect of compression ratio on efficiency at a constant load of 4.0 bar NIMEP is shown in Fig. 35, normalized relative to a compression ratio of 9.8:1. Efficiency improves approximately 2.5% per unit compression ratio. Efficiency peaks at a compression ratio of about 14 to 15:1 with a maximum benefit of 6-7%. This agrees with existing data [5]. Efficiency improves more with compression ratio at high speeds due to the reduced importance of heat loss.

Figures 36 and 37 show the effect of compression ratio on efficiency for various loads at stoichiometric conditions and lambda of 1.3, respectively. Efficiency again improves more with load due to the reduced importance of heat loss, and a reduced pumping loss. The data also shows that load has a higher impact on efficiency under lean conditions than at stoichiometric conditions. As already explained, this occurs because the impact of reduced burn durations, due to higher loads, has a greater effect on efficiency at lean conditions, than at stoichiometric conditions [3].

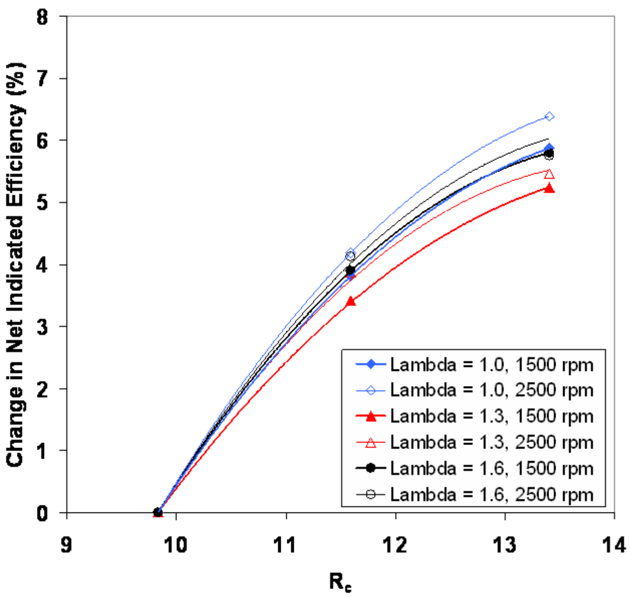

Fig. 35 - Normalized change of net indicated efficiency with compression ratio; 4.0 bar NIMEP

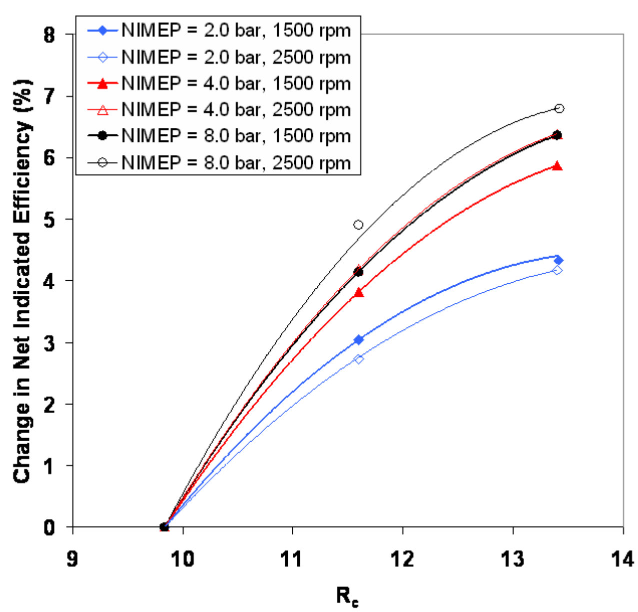

Fig. 36 - Normalized change of net indicated efficiency with compression ratio; lambda=1.0

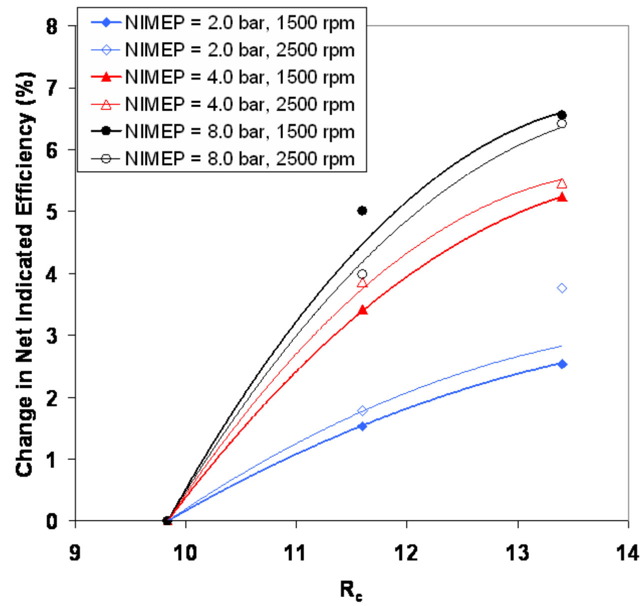

Fig. 37 - Normalized change of net indicated efficiency with compression ratio; lambda=1.3

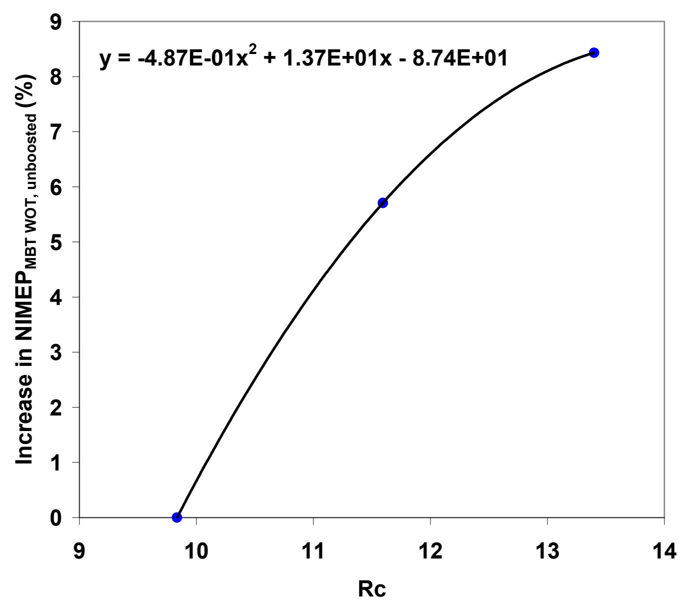

Fig. 38 – Normalized average increase of WOT NIMEP at MBT timing with Rc; lambda=1.0, 1500 RPM

Figure 38 shows the effect of compression ratio on the percentage increase in NIMEP at MBT spark timing and stoichiometric Wide Open Throttle (WOT) conditions. The behavior is similar to that of mid-load efficiency; extrapolating the curve, the maximum NIMEP increase is about 9% at a compression ratio of about 14:1. The equation for the quadratic curve fit is:

$$\frac{NIMEP_{MBT}}{NIMEP_{MBT,9.8:1}} = 0.126 + 0.137R_c - 0.00487R_c^{\,2}$$

SUMMARY AND CONCLUSION

The conclusions from this study can be summarized as follows:

- An extensive data set was generated to study the effects of spark retard, air-fuel ratio, compression ratio, and load on efficiency. Simulations were also performed to provide fundamental explanations for the changes in efficiency.

- A new combustion phasing parameter is presented which accurately correlates changes in NIMEP (or torque) with spark retard; this parameter termed "combustion retard" collapses all changes in NIMEP into one universal curve, across a wide range of operating conditions, including different fuels, different compression ratios, different air-fuel ratios, and different levels of plasmatron enhancement.

- A framework was developed for analyzing the effects of air-fuel ratio on engine efficiency. The summation of the individual process effects on efficiency in the framework gives good agreement with the data under a wide range of conditions. The proposed framework is a useful tool that both provides fundamental knowledge about the variation of efficiency with air-fuel ratio, and predicts accurate results.

- A limiting 10-90% burn duration of 30 CAD was found at the location of peak efficiency irrespective of operating conditions; this implies that the 10-90% burn duration determines efficiency, and that combustion deteriorates significantly beyond this 30 CAD offsetting any efficiency gains from thermodynamics effects, reduced pumping work, or reduced heat transfer losses.

- A limiting 0-10% burn duration of 40 CAD was found at a 2% COV of NIMEP; this implies that NIMEP variability and combustion variability is limited by the duration of the flame initiation process, and not by its variability.

- The 10-90% vs. 0-10% relationship shows a consistent monotonically increasing curve with decreasing slope. The specific relationship changes depending on changes in laminar flame speed and turbulence.

- The location of peak efficiency changes relative to the onset of NIMEP variability; the location of these two points is determined by the 10-90% vs. 0-10% burn duration relationship, subject to the constraints of a limiting 10-90% burn duration at peak efficiency, and a limiting 0-10% burn duration at the onset of variability.

- With increasing lambda, NIMEP variability was found to have no impact until after the location of peak efficiency. Beyond this point, variability plays a modest role, due to the asymmetrical distribution of NIMEP and the 10-90% burn duration.

- The maximum impact of variability on engine efficiency under lean conditions was found to be about 2-3%.

- Independent of combustion variability, the fundamental factor that determines the decrease in engine efficiency at high air-fuel ratios is a lengthening burn duration.

ACKNOWLEDGMENTS

The authors gratefully acknowledge the funding for this project provided by ArvinMeritor

REFERENCES

1. Tully, E., Heywood, J., "Lean Burn Characteristics of a Gasoline Engine Enriched with Hydrogen form a Plasmatron Fuel Reformer." SAE 2003-01-0630

2. Heywood, J.B., Internal Combustion Engine Fundamentals, McGraw Hill, New York, 1988

3. Ivanic, Z., Ayala, F., Goldwitz, J., Heywood, J., "Effects of Hydrogen Enhancement on Efficinecy and NOx emissions of Lean and EGR-Diluted mixtures in a SI Engine." SAE 2005-01-0253

4. Goldwitz, J., Heywood, J., "Combustion Optimization in a Hydrogen-Enhanced Lean Burn SI Engine." SAE 2005-01-0251

5. Muranaka, S., Takagi, Y., and Ishida, T., "Factors Limiting the Improvement in Thermal Efficiency of S.I. Engine at Higher Compression Ratio," SAE 870548

6. Ozdor, N., Dulger, M., and Sher, E. "Cyclic Variability in Spark Ignition Engines: A Literature Survey," SAE paper 940987, 1994

7. Hill, P.G., "Cyclic Variations and Turbulence Structure in Spark-Ignition Engines," *Combustion and Flame*, Vol. 72. pp. 73-89, 1988

8. Stein, R., Tachih, C., Lyjak, J., "The Combustion System of the Ford 5.4L 3-Valve Engine," Technical Paper presented at the September 2003, Powertrain Conference, Dearborn MI

9. Chevron Phillips UTG-96, Certificate of Analysis

10. Poulos, S. G., and Heywood, J.B., "The Effect of Chamber Geometry on Spark Ignition Engine." SAE Paper 830587, 1983

11. Cheng, W.K., Hamrin, D., Heywood, J.B., Hochgreb, S., Min, K, and Norris, M., "An Overview of Hydrocarbon Emissions Mechanisms in Spark-Ignition Engines," SAE paper 932708, presented at the SAE Fuels and Lubricants Meeting and Exposition, Philadelphia, PA, October 18-21, SAE Trans., Vol. 102, 1993.

CONTACT

Ferrán Ayala is a Doctoral Candidate in Mechanical Engineering at the Massachusetts Institute of Technology. He can be reached at ferran@mit.edu

DEFINITIONS, ACRONYMS, ABBREVIATIONS

Lambda, λ: relative air-to-fuel ratio

NIMEP: Net Indicated Mean Effective Pressure; the ratio of the net work per cycle to the cylinder volume displaced per cycle [2]

MBT: Maximum Brake Torque (MBT) timing

Rc: Compression Ratio

ATC: After Top dead Center

COV: Coefficient of Variation

WOT: Wide Open Throttle

APPENDIX

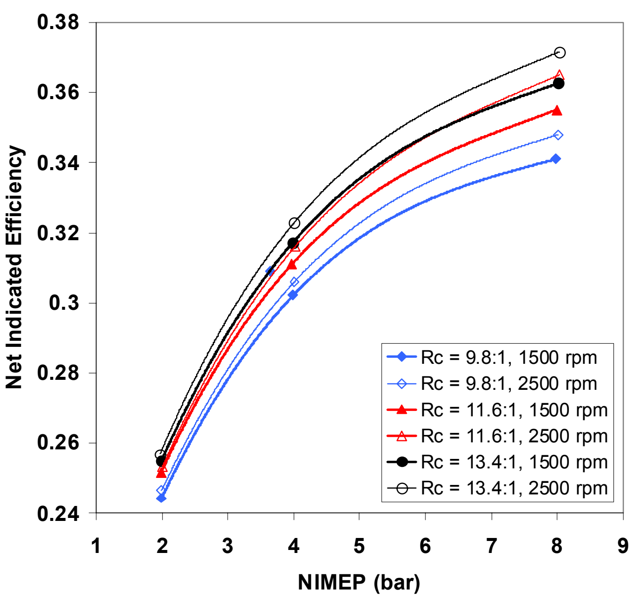

Fig. A.1 – Change of net indicated engine efficiency with NIMEP; lambda=1.0

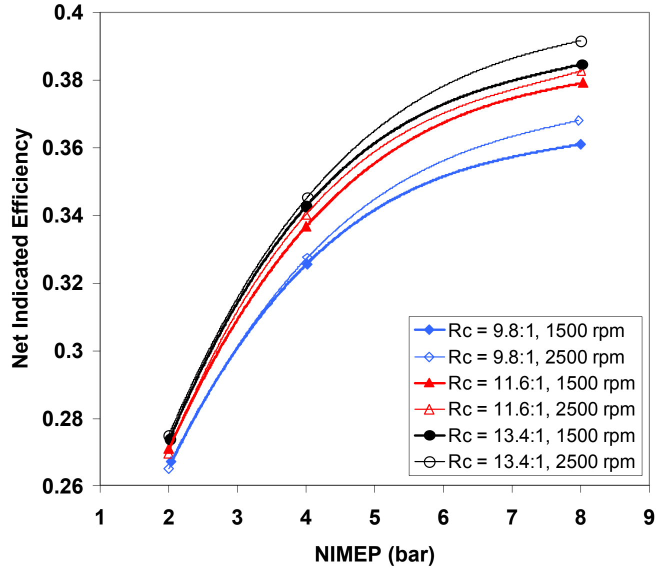

Fig. A.2 – Change of net indicated engine efficiency with NIMEP; lambda=1.3

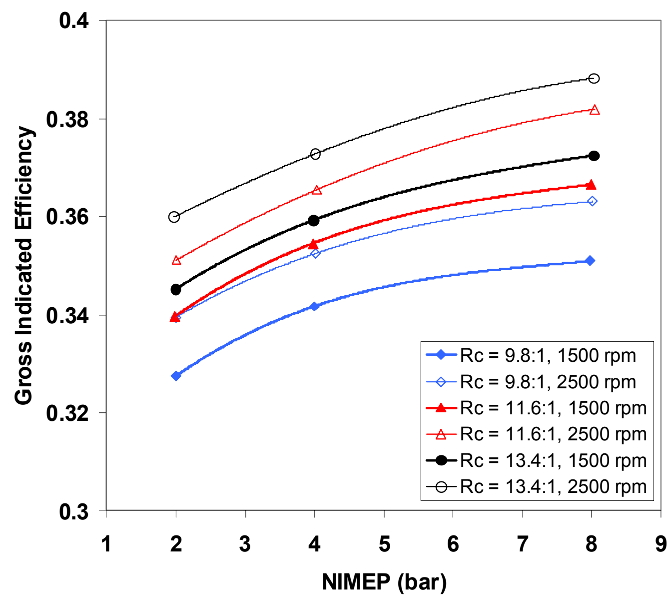

Fig. A.3 – change of gross indicated engine efficiency with NIMEP for a range of compression ratios; lambda=1.0

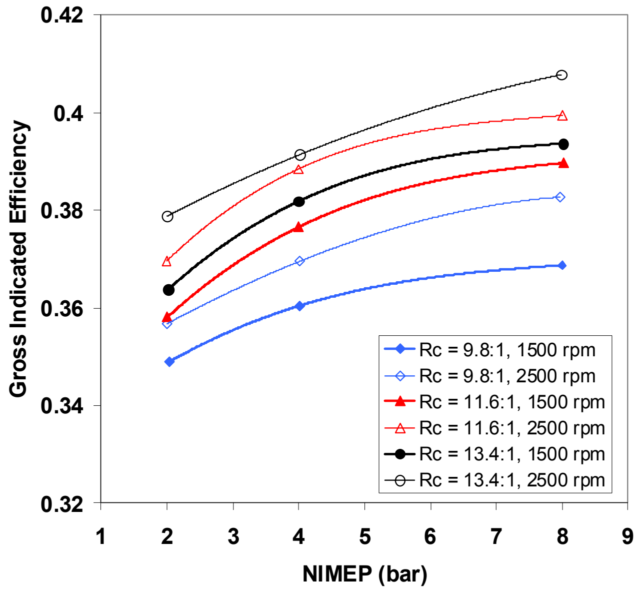

Fig. A.4 – Change of gross indicated engine efficiency with NIMEP; lambda=1.3

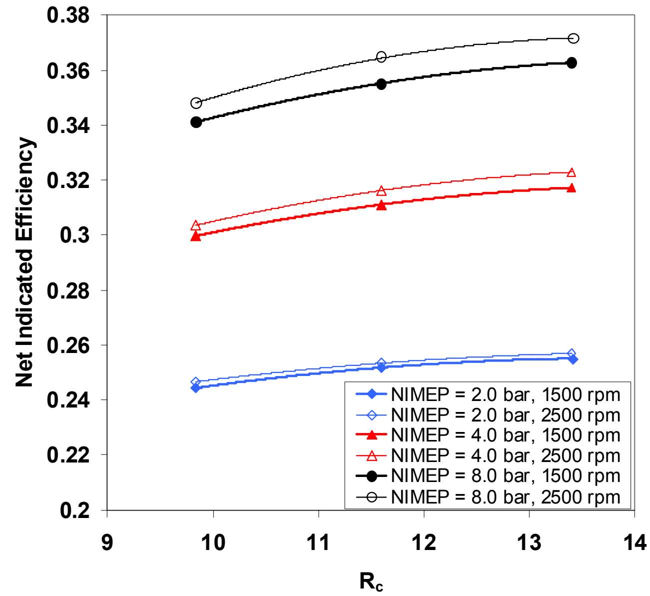

Fig. A.6 – Change in net indicated efficiency with compression ratio for a range of loads; lambda=1.0.

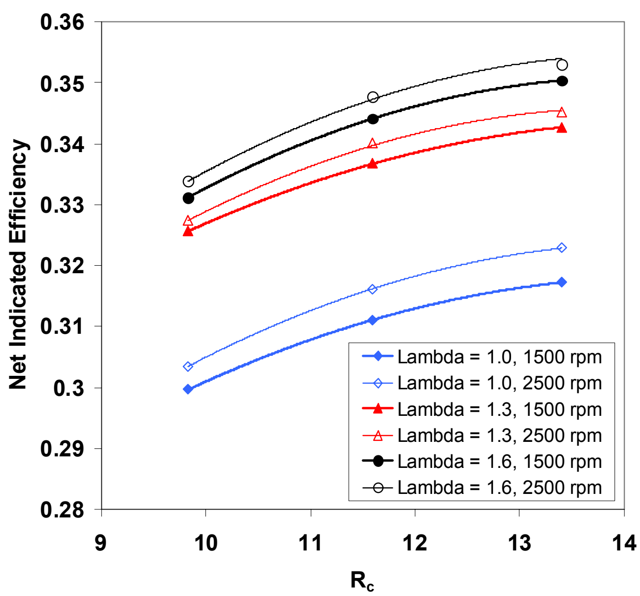

Fig. A.5 – Change of net indicated efficiency with compression ratio for a range of lambda; 4.0 bar NIMEP

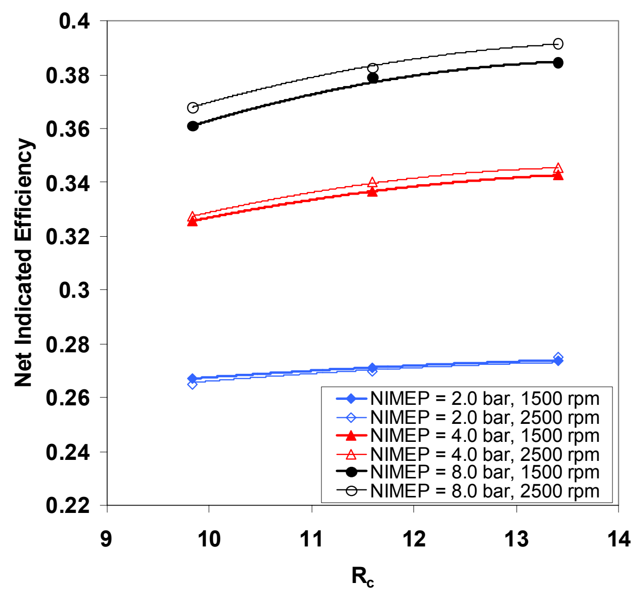

Fig. A.7 – Change in net indicated efficiency with compression ratio for a range of loads; lambda=1.3.